ISSN 1075-7015, Geology of Ore Deposits, 2016, Vol. 58, No. 8, pp. 674–680. © Pleiades Publishing, Ltd., 2016.
Original Russian Text © V.I. Alekseev, Yu.B. Marin, I.M. Gembitskaya, 2015, published in Zapiski Rossiiskogo Mineralogicheskogo Obshchestva, 2015, No. 6, pp. 83–93.

MINERALS AND MINERAL ASSEMBLAGES

Allanite-(Y) and Allanite-(Ce) Paragenesis in Tourmalinite of the Severnyi Pluton, Chukchi Peninsula, and the Relationship between Yttrium and Lanthanides in Allanite

V. I. Alekseev*, Yu. B. Marin, and I. M. Gembitskaya

Saint-Petersburg Mining University, Dvadtsat' pervaya liniya 2, St. Petersburg, 199106 Russia

**e-mail: via@spmi.ru*

Received September 8, 2015

Abstract—The morphology, optical properties, and composition of allanite-(Ce) and allanite-(Y) from rare-metal tourmalinite of the Severnyi granitic pluton in the Chukchi Peninsula have been studied, as well as the composition and structure of host metasomatic rocks and the assemblage of rock-forming and accessory minerals. The hydrothermal origin of both allanite species and their stable combination have been established. Allanite-(Y) is partly replaced with allanite-(Ce), and metasomatic rims 2–10 μm wide enriched in LREE around allanite-(Y) have been identified. The degree of isomorphic Y+HREE substitution for LREE is estimated at 16%, on average; the maximum (Y+HREE)/LREE ratio does not exceed 0.25. It is assumed that the transition of allanite-(Y) into allanite-(Ce) might be caused by anincrease in acidity and decrease in aqueous fluid temperature at the late stage of the hydrothermal process.

Keywords: allanite-(Y), allanite-(Ce), yttrium, lanthanides, paragenesis, isomorphism, tourmalinite, Chukotka

DOI: 10.1134/S107570151608002X

INTRODUCTION

Minerals of the allanite subgroup are the most important concentrators of REE in the Earth's crust. Allanite species and varieties enriched in LREE, especially allanite-(Ce), are acutely predominant in felsic and alkaline igneous, metamorphic, and hydrothermal rocks. Allanite enriched in Y and HREE is extremely rare and occurs mainly in granitic pegmatite and rare-metal granite (Khvostova, 1962; Mineev, 1969; Semenov, 2001; Giere and Sorensen, 2004; Alekseev and Marin, 2012). It has been established that accessory allanite-(Ce) and allanite-(Y) are related to leucogranite and rare-metal granite in the Russian Far East (Alekseev and Marin, 2014; Alekseev, 2014). Therefore, the combination of both aforementioned minerals in the same rock described in this paper is of undoubted interest.

CHARACTERIZATION OF ALLANITE

A quartz–tourmaline vein with high-grade REE mineralization, including allanite-(Ce) and allanite-(Y), has been revealed in an outcrop of granite pertaining to the Severnyi pluton at one of the southern spurs of the Shelag Range in the Chaun District of the Chukchi Peninsula. The metasomatic vein is localized in the zone of tourmalinized granite at the flank of the Kekurny tin deposit. Granite at this outcrop underwent intense tourmaline–albite alteration and was transformed at the contact with the vein into blastogranitic albitite containing admixture (<10%) of quartz, tourmaline, fluorite, and sporadic apatite, thorite, zircon, allanite-(Ce) and allanite-(Y) disseminations. The studied vein is composed of medium-grained (0.2–1.0 mm) granoblastic quartz 1 with abundant (25–60%) poikilitic tourmaline segregations. The early tourmaline generation is represented by large prismatic schorl pale blue in color with dark blue and brown zones. The late generation is characterized by greenish blue acicular schorl. The tourmaline–quartz aggregate contains impregnations (1–5%) of purple subhedral fluorite crystals 200–1200 μm in size and short-prismatic fluorapatite 10–400 μm across mostly in relatively coarse-grained spots of matrix with the predominance of late quartz 2 and a lowered content of tourmaline 2. Tourmalinite and wall-rock albitite contain in order of abundance: allanite-(Ce), apatite-(CaF), fluorite, allanite-(Y), zircon, and thorite. This mineral assemblage is overprinted by low-intense late mineralization: tourmaline is replaced with nontronite, and chains of secondary leucoxene have been noted in substantially quartz spots.

Allanite-(Ce) is identified in gangue tourmaline as numerous reddish brown columnar and acicular crystals with simple rhomb-shaped transverse sections (3–40, occasionally up to 90 μm), which frequently make up

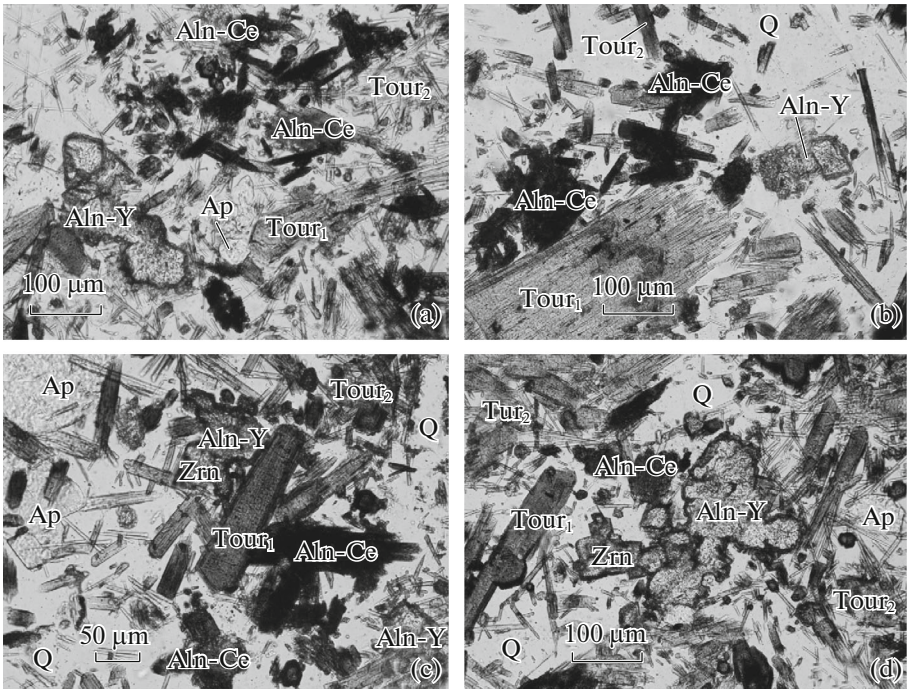

Fig. 1. Coexistence of allanite-(Y) and allanite-(Ce) in tourmalinite from Chaun district of Chukchi Peninsula. Aln-Ce, allanite-(Ce); Aln-Y, allanite-(Y); Ap, apatite-(CaF); Tour, tourmaline; Q, quartz; Zrn, zircon. Micrographs, plane light.

parallel intergrowths. In spots with predominant quartz 2, the content of allanite-(Ce) increases and this mineral is gathered into radiaxial bunches and irregular monomineralic intergrowths up to 0.6 mm in size. Allanite-(Ce) also occurs as inclusions in quartz 2, is closely intergrown with tourmaline 2, apatite, and zircon, and locally replaced with microgranular fluocerite-(Ce) pseudomorphs (Figs. 1, 2).

The optical properties of allanite-(Ce) in transmitted light are as follows: sharp pleochroism from dark reddish brown along N_g (z, γ) to red-brown with slight greenish hue along N_m (y, β) and pale brown to yellowish along N_p (x, α) ($N_g \geq N_m > N_p$); $N_g - N_p \sim 0.022$; dispersion of optical axes is distinct. The chemical composition of allanite-(Ce) is characterized by markedly elevated Fe, Ca contents and deficiency in lanthanides. This composition is close to that of accessory allanite from leucogranite in the Russian Far East but differs in Ti, Mg, Mn deficiency and low Th content. In the crystal chemistry aspect, allanite-(Ce) is distinguished by elevated concentration of silicon–oxygen tetrahedra (3.15–3.48 apfu), which is compensated by vacancy in *A2* hollows (Y, REE) (0.7 apfu, on average). Iron (1.21–1.51 apfu) apparently occupies not only *M3* octahedra, but also *M1*. This allows us to suggest the occurrence of Fe^{3+} (Table 1, columns 1–5). The empirical formula of allanite-(Ce) is $Ca(Ca_{0,17}Ce_{0,43}REE_{0.27})_{0.87}(Al_{1.58}Fe_{1.34})_{2.92}(Si_{3.28}O_{11})O(OH)$.

Allanite-(Y) in tourmalinite yields in abundance to allanite-(Ce), is distributed throughout the vein, and its amount somewhat increases in selvages. The mineral is intimately intergrown with tourmaline of both generations and quartz 1, occasionally with fluorite, and is infrequently aggregated with apatite. Allanite-(Y) is characterized by euhedral short-prismatic crystals 15–50 μm and occasionally 95–115 μm in size. Monomineralic polycrystalline intergrowths of allanite-(Y) up to 0.1–0.4 mm in size are typical (Figs. 1, 2). Crystals with a block structure and polysynthetic twins oriented across elongation are noted. The optical properties of allanite-(Y) are as follows: colorless, with a secondary yellow-brown rim; $N_g - N_p = 0.009$–0.011, and appreciable dispersion.

The chemical composition of allanite-(Y) is distinguished by an extremely low Al content, elevated Ca and Y concentrations (Table 1, columns 6–9). These features make allanite-(Y) similar to accessory analogs in Li–F granites from the Russian Far East (Alekseev, 2014). The empiric formula of allanite-(Y) is $Ca(Ca_{0.22}Y_{0.78}) \times (Al_{0.10}Fe_{0.88}Y_{1.67}REE_{0.62})_{3.27}(Si_{2.81}O_{11})O(OH)$. As compared with allanite-(Ce) from the same tourmalinite, the mineral is sharply depleted in Fe and especially in Al; Fe/Al = 8.8; for comparison, this ratio in allanite-(Ce) is ~0.9 (Table 1). The main crystal chemical feature of allanite-(Y) is unstable distribution of Y and lanthanides between sites)*A* and *M*, as was previously noted for accessory allanite in Li–F granite (Alekseev et al., 2012); the deficiency in Al and Fe in *M*-octahedra is about 2.02 apfu; and the superfluous amount of Y + REE cations at site *A* reaches 2.20 apfu.

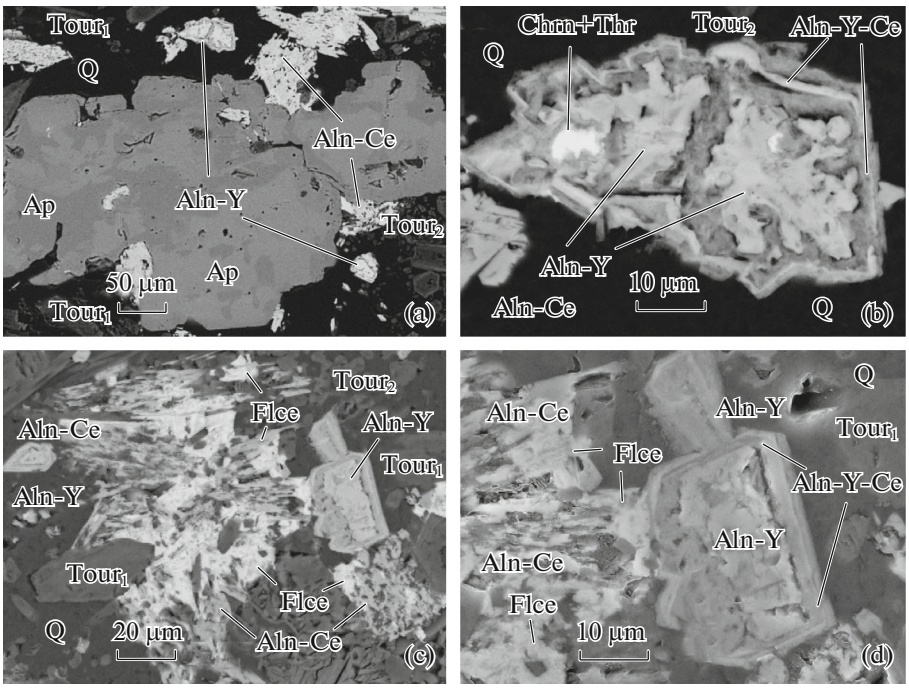

Fig. 2. Anatomy of allanite-(Y) and allanite-(Ce) aggregates and individuals in tourmalinite from Chaun District of Chukchi Peninsula: (a) parallel intergrowths of columnar allanite-(Ce) and intergrowths of allanite-(Y) at contacts with fluorapatite; (b) close-up of allanite-(Y) with secondary chernovite, thorite, and Y–Ce rim; (c) contact of radiaxial intergrowth of columnar allanite-(Ce) crystals partly replaced with fluocerite with parallel short-prismatic allanite-(Y) crystals; (d) close-up image of allanite-(Y) with Y–Ce rim. Aln-Y-Ce, allanite (Y,Ce); Chrn, chernovite-(Y); Thr, thorite; Flce, fluocerite. See Fig. 1 for other letter symbols; (a–c) BSE images; (d) image in secondary electrons.

RELATIONSHIP BETWEEN ALLANITE-(Y) AND ALLANITE-(Ce)

Allanite-(Ce) and allanite-(Y) crystals occur in tourmaline–quartz aggregates as monominerallic segregations localized close to each other. In many cases, these segregations come in contact and display reaction relationships, where faces of euhedral allanite-(Y) crystals become distorted and corroded (Figs. 2c, 2d; 3b–3d); the crystals contain secondary chernovite-(Y) and thorite inclusions (Fig. 2b). In segregations of allanite-(Ce), the relics of its yttrium precursors (Figs. 3a, 3d) are detected. It can be suggested that allanite-(Ce) forms later than allanite-(Y) and partly replaces the latter.

Along with aggregative replacement of allanite-Y with its cerium proxy, outer rims 2–10 μm wide enriched in LREE are widespread. They are apparently products of diffusion metasomatic transformation of allanite-(Y) and represent incomplete pseudomorphs of allanite-(Ce) after allanite-(Y) (Figs. 1a–1d; 2b, 2d; 3b). The intermediate composition of rims indicates incomplete diffusion exchange of HREE and LREE apparently related to their distinct sites in the allanite crystal structure (Table 2).

Figure 4a shows the typical zoning of allanite-(Y) crystal caused by cation exchange in the course of its metasomatic alteration. Unaltered allanite-(Y) has been identified in the core (data points 5, 6 in probe profile). The outer rim (data points 1–4, 7–9) is characterized by depletion in Y and HREE and by enrichment in Ce, Nd, and Sm (Fig. 4b).

The metasomatic rims, as a rule, are composed of three to four zones differing in diffusion intensity. The main trend is the gain of LREE, Si, Al, Th and the loss of Y, HREE, Fe, and Ca (compare column 9 in Table 1 and column 7 in Table 2). The formula coefficient ratio LREE/(Y + HREE) varies, on average, from 0.04/2.18 in cores to 0.16/1.34 in rims. The amount of Si cations markedly increases from core to periphery of allanite-(Y) (from 3.59 to 4.31 apfu); Al contents also somewhat increase and Th appears (0.05 apfu). The outermost zone of rim a few μm wide is depleted in all lanthanides and occasionally enriched in Fe up to 26.09–34.37 wt %.

The restricted LREE–(Y + HREE) isomorphism in minerals from allanite subgroup was earlier noted by Khvostova (1962), Mineev (1969), Giere and Sorensen (2004), etc. Two-step REE isomorphism in allanite-(Y) has been established (Alekseev et al., 2012). The reason for incomplete HREE and LREE miscibility may be their separate positions in the crystal structure and metastable character of the allanite structure proper. The elevated Y and HREE content in the altered allanite shows that replacement of these

Table 1. Chemical composition (wt %) of allanite-(Ce) and allanite-(Y) from tourmalinite of Chukchi Peninsula

Component	Allanite-(Ce)					Allanite-(Y)				
	1	2	3	4	5	6	7	8	9	10
SiO_2	35.55	37.59	35.54	35.28	35.83	35.61	33.97	35.22	35.79	33.85
Al_2O_3	14.42	13.91	13.53	14.43	14.22	–	0.83	0.42	0.54	1.41
FeO*	17.37	15.61	19.18	17.27	18.37	9.38	8.88	7.72	8.94	12.23
CaO	12.59	9.72	14.15	11.75	9.62	12.31	10.66	8.06	10.56	3.09
La_2O_3	4.69	4.84	4.82	4.99	4.42	–	–	–	–	0.07
Ce_2O_3	11.28	13.61	12.47	12.63	11.57	–	0.27	–	0.06	3.07
Nd_2O_3	3.81	3.41	2.68	3.05	3.16	–	0.69	1.15	0.54	3.96
Sm_2O_3	–	–	–	–	0.03	–	1.83	0.89	0.54	1.73
Gd_2O_3	–	–	–	–	–	–	1.42	3.12	0.86	3.65
Dy_2O_3	–	–	–	–	–	–	3.55	3.83	1.61	4.32
Er_2O_3	–	–	–	–	–	–	3.45	–	0.51	2.94
Yb_2O_3	–	–	–	–	–	–	2.89	–	0.42	2.14
Y_2O_3	–	–	–	–	0.11	42.34	30.77	38.05	38.69	27.19
ThO_2	–	–	–	0.01	1.55	–	–	–	0.03	0.30
Total	99.71	98.69	100.39	99.41	99.97	99.64	99.21	98.47	99.09	100.23
Formula coefficients of cations										
Si	3.28	3.48	3.15	3.28	3.31	3.53	3.55	3.63	3.59	3.62
Al	1.57	1.52	1.50	1.58	1.55		0.10	0.05	0.06	0.18
Fe*	1.34	1.21	1.51	1.34	1.42	0.78	0.78	0.67	0.75	1.09
Σ*M*	2.91	3.03	3.01	2.92	3.05	0.78	0.88	0.72	0.81	1.29
Ca	1.25	0.96	1.42	1.17	0.95	1.31	1.19	0.89	1.14	0.35
La	0.16	0.17	0.17	0.17	0.15					0.00
Ce	0.38	0.46	0.43	0.43	0.39		0.01		0.00	0.12
Nd	0.13	0.11	0.09	0.10	0.10		0.03	0.04	0.02	0.15
Sm					0.00		0.07	0.03	0.02	0.06
Gd							0.05	0.11	0.03	0.13
Dy							0.12	0.13	0.05	0.15
Er							0.11		0.02	0.10
Yb							0.09		0.01	0.07
Y					0.01	2.23	1.71	2.09	2.07	1.55
Th				0.00	0.03				0.00	0.01
Σ*A*	1.92	1.70	2.11	1.87	1.63	3.54	3.38	3.29	3.36	2.69

(1–3, 6–8) Representative allanite-(Ce) and allanite-(Y) microprobe analyses, respectively, from tourmalinite; analyses were performed at Saint-Petersburg Mining University, St. Petersburg; (4, 9) mean allanite-(Ce) and allanite-(Y) compositions of 33 and 12 analyses, respectively; (6, 7) mean accessory allanite-(Ce) and allanite-(Y) compositions of 328 and 86 analyses, respectively, from leucogranites and Li–F granites of Russian Far East. Accessory allanite also contains, wt %: (5) 0.07 MgO, 0.95 TiO_2, 0.06 MnO; (10) 0.26 MnO. Dash indicates that element was not detected; FeO* = FeO + Fe_2O_3. Formula coefficients were recalculated based on 8 cations with equilibration for 12.5 oxygen ions, after Ercit (2002).

elements with LREE occurs largely at site *A2*, whereas HREE are partly incorporated into *M*-octahedrons. Calculations have shown that the degree of Y and HREE replacement with LREE is 16%, on average, and the maximum (Y + HREE)/LREE ratio in the rims of allanite-(Y) does not exceed 25%

DISCUSSION ON ALLANITE-(Y) AND ALLANITE-(Ce) COEXISTENCE PHENOMENON

First of all, the hydrothermal metasomatic origin of the described mineral assemblage should be noted. The hydrothermal allanite-(Y) was almost unknown

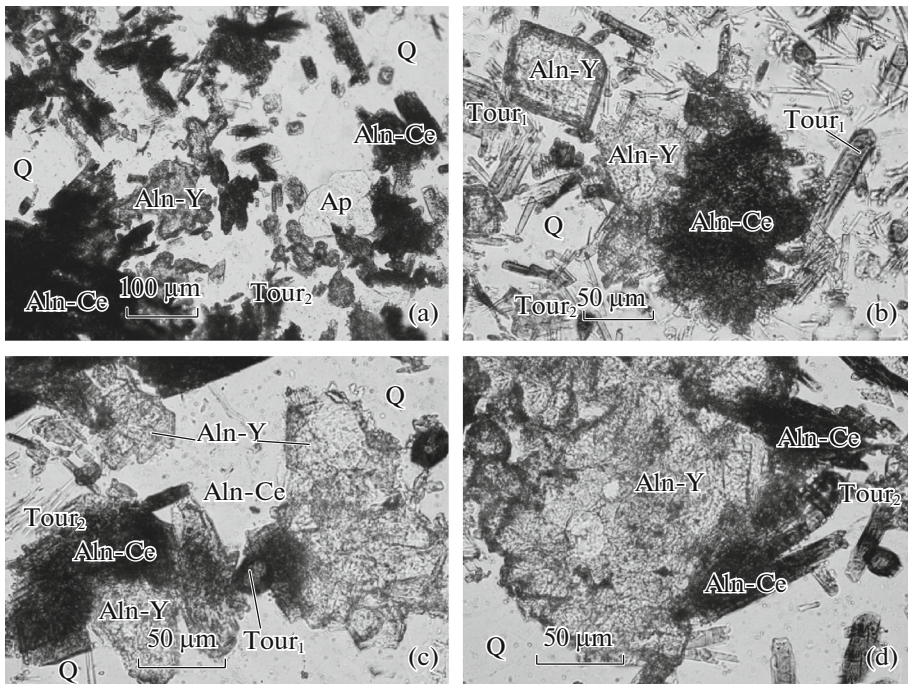

Fig. 3. Relationships between allanite-(Y) and allanite-(Ce) in tourmalinite from Chaun District of Chukchi Peninsula. Micrographs, plane light. See Fig. 1 for letter symbols.

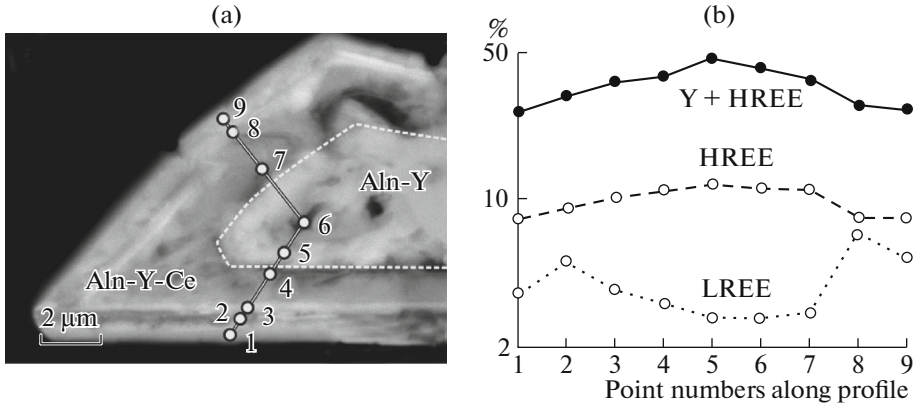

Fig. 4. (a) Allanite-(Y) (Aln-Y) with secondary Y–Ce rim (Aln-Y–Ce) from tourmalinite. BSE image; (b) distribution of yttrium and lanthanides along microprobe profile 1–9. Close-up of Fig. 2c.

until now. Its first find was probably done by Nel et al. (1949) in Sn-bearing tourmalinite from Transvaal. Thereby REE composition was not studied, and the found mineral had been called lombardite. Later on, Y and Nd had been detected: 5.49 and 5.81 wt %, respectively (Neumann and Nilssen, 1962). Semenov (2001) mentioned "yttro-orthite" in greisen from the Iul'tin tin deposit of the Chukchi Peninsula.

Since no indications of staged formation of the basic mineral assemblage (albite–quartz–fluorite–apatite–zircon–thorite–allanite-(Ce)–allanite-(Y)) are known, we can conclude that allanite-(Ce) and allanite-(Y) can make up paragenesis in the understanding of Korzhinsky (1957), Betekhtin (1958), and Ivanov (1972): a combination of minerals characterized by their coeval formation as products of the same stage of a certain process. Allanite-(Ce) forms somewhat later and partly replaces allanite-(Y). The joint formation of allanite-(Ce) and allanite-(Y) is a unique phenomenon. We do not know other cases of such paragenesis, however, judging from the literature sources, hydrothermal or hydrothermally altered allanite is characterized by fluctuation in the proportions of LREE and HREE (Exley, 1980; Meintzer and Mitchell, 1988; Galankina et al., 1998; Wood and

Table 2. Chemical composition (wt %) of metasomatic rims around allanite-(Y)

Component	1	2	3	4	5	6	7
SiO_2	42.97	45.56	47.08	43.86	36.63	48.84	45.08
Al_2O_3	—	1.21	3.40	1.02	1.68	0.26	1.06
FeO*	7.20	9.80	6.74	7.68	8.90	5.07	7.20
CaO	8.56	7.70	7.18	7.37	9.21	5.55	7.67
Ce_2O_3	—	—	0.75	0.40	1.39	0.94	0.51
Nd_2O_3	3.95	2.34	1.33	1.84	1.80	3.18	2.22
Sm_2O_3	—	1.99	1.68	2.91	1.54	2.86	1.69
Gd_2O_3	—	2.19	2.42	3.12	2.52	2.82	2.29
Dy_2O_3	—	3.34	3.57	3.29	4.34	2.48	2.83
Er_2O_3	—	—	0.41	1.92	2.58	1.37	1.32
Yb_2O_3	—	—	1.80	3.10	1.79	1.73	1.43
Y_2O_3	25.18	23.11	18.27	19.39	24.87	19.40	21.69
ThO_2	9.87	—	2.28	1.38	1.35	1.73	2.27
Total	97.74	97.25	96.91	97.29	98.61	96.25	97.26

(1–6) Representative microprobe analyses of allanite rims; (7) mean allanite rim composition of 10 analyses. See notes to Table 1 for analytical conditions.

Ricketts, 2000; Čobić et al., 2010; Zenina and Konovalenko, 2012), including allanite from tourmalinite (Nel et al., 1949; Campbell et al., 1984).

Allanite-(Ce) versus allanite-(Y) antagonism is caused by variable alkalinity and composition of volatile components in magmatic melts. Increase in alkalinity and saturation with fluid at the final stages of granitic magmatism gives rise to the gain of REE in the residual melt and fractionation of HREE and LREE (Balashov, 1976; Alekseev et al., 2012). In magmatic systems with Li–F granites, in particular, in the Severnyi granitic pluton, Y and HREE are retained in the fluid phase and crystallize in rare-metal granite and associated zwitter as various minerals, e.g., allanite-(Y), fergusonite-(Y), chernovite-(Y), aeschynite-(Y), tveitite-(Y), britholite-(Y), gadolinite-(Y), polycrase-(Y), etc. (Alekseev, 2014). The tendency toward a gain of Y and HREE and the probability of allanite-(Y) formation should increase at the early postmagmatic stage for an elevated alkalinity and fluorine fugacity (Alekseev and Marin, 2012). In the course of subsequent hydrothermal processes, including tourmalinization, the change in F^- for Cl^-, B^{3-} and the drop in temperature control the inversion of REE pattern, accumulation of LREE, and allanite-(Ce) formation (Balashov, 1976).

It is suggested that the alkaline setting characteristic of the albite–tourmaline stage of metasomatism in granites of the Severnyi pluton, gave way to acidic conditions at the end of this stage. As a result, the metasomatism gradually changes: albite–quartz (1)–tourmaline (1)–allanite-(Y) → quartz (2)–tourmaline (2)–zircon–fluorapatite–fluorite–allanite-(Ce). Thus, variation of acidity–alkalinity in the flow of the hydrothermal solution creates conditions for the formation of such geochemically distinct minerals as allanite-(Y) and allanite-(Ce).

CONCLUSIONS

(1) The hydrothermal origin of allanite-(Y) has been established.

(2) The allanite-(Y) and allanite-(Ce) paragenesis has been established in tourmalinite from the Severnyi granitic pluton in the Chaun District of the Chukchi Peninsula.

(3) A restricted (Y + HREE)–LREE isomorphism in allanite has been recorded.

ACKNOWLEDGMENTS

This study was carried out under the basic and project parts of the state task in the field of scientific activity no. 5.2115.2014/K for 2014–2016 and was supported by the Russian Foundation for Basic Research (project nos. 11-05-00868-a, 14-05-00364).

REFERENCES

Alekseev V.I., Marin Yu.B., Gembitskaya I.M. Allanite-(Y) in areas of ongonite magmatism in the Far East: Isomorphism and petrogenetic implications, *Geol. Ore Deposits*, 2013, vol. 55, pp. 503–514.

Alekseev, V.I. and Marin, Yu.B., Chernovite-(Y) and other arsenic minerals in rare-metal granites and greisens of the Far East, *Geol. Ore Deposits*, 2013, vol. 55, pp. 601–606.

Alekseev, V.I., *Litii-ftoristye granity Dal'nego Vostoka,* (Lithium-Fluoric Granites of the Far East) Saint Petersburg: National Mineral Resources University, 2014.

Alekseev, V.I. and Marin, Yu.B., Accessory mineralization of rocks from Late Cretaceous intrusive series with Li-F granite in the Far East, *Geol. Ore Deposits*, 2015, vol. 57, pp. 537–551.

Balashov, Yu.A., *Geochemistry of the Rare-Earth Elements*, Moscow: Nauka, 1976.

Campbell, F.A. and Ethier, V.G., Composition of allanite in the footwall of the Sullivan orebody, British Columbia, *Can. Mineral.*, 1984, vol. 22, pp. 507–511.

Čobić, A., Bermanec, V., Tomašić, N., and Škoda, R., The hydrothermal recrystallization of metamict allanite-(Ce), *Can. Mineral.*, 2010, vol. 48, pp. 513–521.

Ercit, T.S., The mess is "allanite", *Can. Mineral.*, vol. 40, pp. 1411–1419.

Exley, R.A., Microprobe studies on REE-rich accessory minerals; implications for Skye Granite petrogenesis and REE mobility in hydrothermal systems, *Earth Planet. Sci. Lett.*, 1980, vol. 48, pp. 97–110.

Galankina, O.L., Gavrilenko, V.V., and Gaydamako, I.M., New data on mineralogy of the hydrothermal gold-PGE mineralization at the Polar Urals, *Zap. Vseross. Mineral. O-va*, 1998, no. 3, pp. 72–78.

Gieré, R. and Sorensen, S.S., Allanite and other REE-rich epidote-group minerals. Epidotes. *Rev. Miner. Geochem.*, 2004, vol. 56, pp. 431–493.

Ivanov, O.P., Some remarks to definition of concepts "paragenesis", "mineralgeneration" and "mineralization stage", *Zapiski Vseross. Mineral. O-va*, 1972, no. 5, pp. 329–336.

Khvostova, V.A., Mi*neralogy of Orthite. Proc. Inst. Mineral. Geochem. Crystallochem. Rare Elements*, Moscow: Acad. Nauk SSSR, 1962, No. 8.

Meintzer, R.E. and Mitchell, R.S., The epigene alteration of allanite, *Can. Mineral.*, 1988, vol. 26, pp. 945–955.

Mineev, D.A., *Lantanoidy v mineralakh,* (Lanthanides in Minerals), Moscow: Nedra, 1969.

Nel, H.J., Strauss, C.A., and Wickmann, F.E., Lombaardite, a new mineral from the Zaaiplaats tin mine, Central Transvaal, *Union South Africa, Dept. Mines, Geol. Surv. Mem.*, 1949, no. 43, pp. 45–57.

Neumann, H. and Nilssen, B., Lombaardite, a rare earth silicate, identical with, or very closely related to allanite, *Norsk. Geol. Tidsskrift*, 1962, vol. 42, no. 3, pp. 277–286.

Semenov, E.I., *Orudenenie i mineralizatsiya redkikh zemel, toriya, I urana* (*lantanidov i aktinidov*) (Ore and Mineralization of the Rare Earths, Thorium, and Uranium (Lanthanides and Actinides), *Moscow: GEOS*, 2001.

Wood, S.A. and Ricketts, A., Allanite-(Ce) from the Eocene Casto granite, Idaho: response to hydrothermal alteration, *Can. Mineral.*, 2000, vol. 38, pp. 81–100.

Zenina K.S. and Konovalenko S.I., Orthite of the Tsakhirinsky rare-metal occurrence (the Western Mongolia), in *Mineralogy, Geochemistry, and Mineral Resources of Asia*, Tomsk: Tomsk CSTI - branch FGBU CEA Russian Ministry of Energy, 2012, vol. 2, pp. 46–51.

Translated by V. Popov